

## Femtosecond pulsed laser induced damage characteristics on Si-based multi-layer film

ZHENG Chang-bin<sup>1\*</sup>, SHAO Jun-feng<sup>1</sup>, LI Xue-lei<sup>1</sup>, WANG Hua-long<sup>1</sup>,  
WANG Chun-rui<sup>1</sup>, CHEN Fei<sup>1</sup>, WANG Ting-feng<sup>1,2</sup>, GUO Jin<sup>1</sup>

(1. *State Key Laboratory of Laser Interaction with Matter, Changchun Institute of Optics, Fine Mechanics and Physics, Chinese Academy of Sciences, Changchun 130033, China;*

2. *University of Chinese Academy of Sciences, Beijing 100049, China)*

\* *Corresponding author, E-mail: zhengchangbin@ciomp.ac.cn*

**Abstract:** In order to understand the ultrafast laser-induced damage mechanisms of typical imaging sensor's film structures, the damage characteristics of Si-based multi-layer films irradiated by a femtosecond pulsed laser were investigated, and the laser pulse fluence ranges and threshold conditions corresponding to various damage phenomena were evaluated. Si-based multi-layer films that were similar in structure of CCD were prepared by electron beam deposition. The damage characteristics of these films irradiated by a femtosecond pulsed laser with wavelength of 800 nm and pulse width of 100 fs under different pulse fluences and numbers were investigated using a metallurgical microscope. Experimental results showed that the laser-affected zone size increased linearly with pulse fluence in the range of 1.01 to 24.7 J/cm<sup>2</sup>. Surface damage caused by oxidation/amorphization, non-thermal ablation, and laser-induced plasma ablation could be observed in the laser irradiated zone, which tightly depended on the pulse fluence. Multi-layer damage could be observed and the damage probability increased from 1% to 51% in the pulse fluence range from 2.42 to 24.7 J/cm<sup>2</sup>. Irradiated by sequent pulses at a fluence of 1.01 J/cm<sup>2</sup>, the laser affected zone remained almost unchanged and the ablated depth increased with the pulse number. From the single pulse damage experiment data, the femtosecond pulse laser-induced surface damage threshold was evaluated to be 0.543 J/cm<sup>2</sup> and laser-induced multi-layer stress damage threshold was linearly fitted to be 2.16 J/cm<sup>2</sup>. Sequent pulse irradiation with low fluence ( $\leq 1.01$  J/cm<sup>2</sup>) also could lead to deep damage on the multi-layer film.

**Key words:** laser ablation; laser damage; Si-based multi-layer film; damage threshold

收稿日期:2018-01-23;修订日期:2018-03-20

基金项目:激光与物质相互作用国家重点实验室自主基金课题(No. SKLLIM-1502)

Supported by Fundamental Research Project of Chinese State Key Laboratory of Laser Interaction With Matter (No. SKLLIM-1502)

# 飞秒脉冲激光对硅基多层膜损伤特性

郑长彬<sup>1\*</sup>, 邵俊峰<sup>1</sup>, 李雪雷<sup>1</sup>, 王化龙<sup>1</sup>, 王春锐<sup>1</sup>, 陈飞<sup>1</sup>, 王挺峰<sup>1,2</sup>, 郭劲<sup>1</sup>

(1. 中国科学院 长春光学精密机械与物理研究所

激光与物质相互作用国家重点实验室, 吉林 长春 130033;

2. 中国科学院大学, 北京 100049)

**摘要:**为了明确超快激光损伤典型成像探测器膜层结构的物理机制,对飞秒脉冲激光辐照硅基多层膜的损伤特性,以及各种损伤效应对应的激光能量通量范围和阈值条件进行研究。利用波长为 800 nm、脉冲宽度为 100 fs 的脉冲激光和金相显微镜研究了硅基多层膜在不同激光能量通量和不同脉冲累积下的损伤效应。在能量通量为 1.01 ~ 24.7 J/cm<sup>2</sup> 的激光单脉冲辐照下,激光作用区域可观察到氧化/无定形化、非热烧蚀和激光诱导等离子体烧蚀所引起的表面损伤,其损伤效应与激光能量通量有明显联系,激光作用区域尺寸随能量通量线性增大。在 2.42 J/cm<sup>2</sup> 到 24.7 J/cm<sup>2</sup> 激光能量通量范围内,可在辐照表面观察到激光诱导压力导致的多层损伤,损伤概率随激光能量通量的增加由 1% 增大到 51%。在激光能量通量为 1.01 J/cm<sup>2</sup> 的连续多脉冲辐照下,烧蚀区域尺寸几乎不变,但烧蚀深度逐渐增加,其多层损伤机制为表面损伤的累积效应。通过单脉冲损伤实验数据拟合计算确定,飞秒激光诱导硅基多层膜表面损伤阈值为 0.543 J/cm<sup>2</sup>,应力多层损伤阈值为 2.16 J/cm<sup>2</sup>。低激光能量通量(≤1.01 J/cm<sup>2</sup>)多脉冲辐照累积作用同样可造成硅基多层膜深层损伤。

**关键词:**激光烧蚀;激光损伤;硅基多层膜;损伤阈值

**中图分类号:** TN249 **文献标识码:** A **doi:** 10.3788/CO.20191202.0371

## 1 Introduction

Silicon-based materials have a wide range of applications in the field of visible and near-infrared imaging. It is of great practical value to study the damage and destruction effects on silicon-based materials and the corresponding mechanisms under different laser parameters, including thermal effects, mechanical effects, and electric field effects, and so on<sup>[1-4]</sup>. In the research on the interactions between ultrashort pulse laser and silicon-based materials, many theoretical and experimental studies on the effects of irradiation damage have been carried out both domestically and abroad. In 2002, Bonse *et al.* studied the modification threshold and morphology changes of silicon ablated by femtosecond laser and found that the surface of materials will undergo a series of phenomena such as amorphization, melting, recrystallization, nucleation and burning as the laser energy flux increases<sup>[5]</sup>. In 2004, Jia *et al.* studied

the effects of femtosecond lasers on single crystal silicon film. The results show that when the laser intensity is lower than the ablation threshold, enough heat can still cause the silicon material to be amorphous<sup>[6]</sup>. In 2005, Amer *et al.* compared the stress and structural changes of silicon wafers induced by femtosecond and nanosecond lasers<sup>[7]</sup>. In 2008, Guo Chunfeng *et al.* studied the thermoelasticity of ultra-short pulse laser irradiated silicon film<sup>[8]</sup>. In 2008, Crawford *et al.* studied the damage of laser-irradiated multi-layer film composed of metal, oxide and silicon. Through cross-section testing, it was found that the inner silicon was damaged while the surface protective layer metal was intact<sup>[9]</sup>. In 2011, Yang Hongdao *et al.* studied variations in silicon surface characteristics induced by nanosecond pulsed lasers in different gas environments and discussed the influences of laser pulse accumulation on the morphology of silicon materials<sup>[10]</sup>. In 2012, Rublack *et al.* used pulsed lasers between 20 fs and 2000 fs to irradiate silicon wafers with different

transparent materials. The damage was studied using spectral analysis, atomic force microscopy, scanning electron microscopy, transmission electron microscopy, *etc.* The results show that the damage is derived from the electron hole plasma generated by the ultra-short pulse laser in the surface region of the silicon layer<sup>[3]</sup>. In 2013, Ma Pengfei and others studied the effects of femtosecond laser irradiation from various laser energy fluxes on single crystal silicon<sup>[11]</sup>. In 2014, Qi Litao measured the damage energy threshold of single-crystal silicon with different wavelengths of nanosecond laser in a vacuum<sup>[12]</sup>. In the same year, Shao Junfeng *et al.* studied the thermal damage and non-thermal damage mechanism of femtosecond laser on silicon and analyzed the cumulative damage effect of femtosecond laser<sup>[13]</sup>.

However, the laser parameters used and the preparation methods for the silicon-based materials were different and the damage threshold and mechanism were dissimilar. Of special significance, the reports on laser irradiation characteristics and damage mechanisms for a typical detector's film structure are still relatively few<sup>[14]</sup>. In preliminary work, this laboratory has studied the damage and failure mechanisms of charge coupled devices (CCD) under ultrafast laser irradiation<sup>[15-16]</sup> but the physical mechanisms of the interaction between CCD film structures and ultrafast lasers have not yet been made clear.

Based on the above, this paper studies the effects of damage on Si-based multi-layer film under femtosecond pulsed laser irradiation and focuses on the damage mechanisms of Si-based multi-layer film irradiated by a femtosecond pulsed laser, as well as the laser energy flux range and threshold conditions corresponding to the various damage effect.

## 2 Experiment

A Si-based multi-layer film prepared by electron beam deposition was used as the research object. The thickness and composition of each layer of

the Si-based multi-layer film were simplified with reference to the parameters of a typical back-illuminated CCD photosensitive zone, as shown in Fig. 1. (100) plane single crystal silicon with a thickness of 2 mm was selected as the substrate and high purity silicon (purity 99.999% to 99.999 9%) was used as a film material. 300 nm polysilicon, 200 nm silicon dioxide, and 15  $\mu\text{m}$  single crystal silicon were sequentially deposited under a vacuum of  $3 \times 10^{-3}$  Pa.

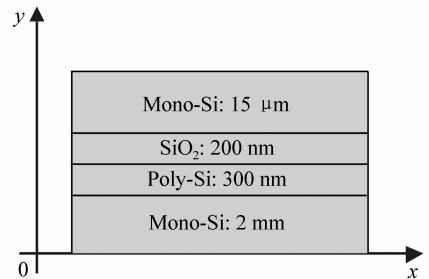


Fig. 1 Sketch of structure for Si-based multi-layer film

图1 硅基多层膜结构示意图

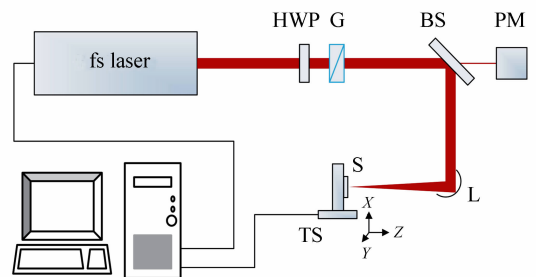


Fig. 2 Schematic of femtosecond laser-induced damage experiment setup, including a Glan prism (G), a half wave plate (HWP), a beam splitting mirror (BS), a power meter (PM), an off-axis parabolic mirror (L), a translation stage (TS) and a sample (S)

图2 飞秒激光诱导损伤的实验装置示意图,图中包括格兰棱镜(G)、半波片(HWP)、分束镜(BS)、功率计(PM)、离轴抛物面反射镜(L)、平移台(TS)和样品(S)

Fig. 2 shows a schematic diagram of the experimental setup of femtosecond laser-induced damage experiment. The laser system used in this experi-

ment was an ultrafast Ti:sapphire amplifier (Coherent Libra). The output laser had a full-width half-height of 50 fs, a wavelength of 800 nm, a repetition rate of 1 kHz or a single trigger, and a maximum single-pulse energy of about 4 mJ. Its beam energy distribution is close to the Gaussian distribution. The laser energy was attenuated to the required level using a pair of grand prisms and half-wave plates and then monitored with an energy meter. Finally, an off-axis polishing mirror was used to focus the laser beam to a spot diameter of approximately 100  $\mu\text{m}$  onto the sample's surface. The sample was mounted on a three-dimensional translation stage that could be programmed by a computer to ensure that each laser pulse acted on a new surface. During the experiment, each time the laser energy was adjusted, 100 ablation points were applied to calculate the probability of damage.

The surface damage of the film was observed using a metallographic microscope. The test equipment used was an EB-4 metallographic microscope from Taiwan Haoye International Co., Ltd. The total magnification of the system was 400 $\times$ .

### 3 Experimental Results and Analysis

#### 3.1 Study of the surface ablation damage effect

##### 3.1.1 Comparison of typical radiation damage morphology

Fig. 3 shows a micrograph of the damage on a single-pulse laser irradiated Si-based multi-layer film's surface. No obvious thermal damage was observed throughout the tunable energy range, confirming that the femtosecond laser is of non-thermal ablation characteristics, which are significantly different from those of the nanosecond laser. Generally, the melting phenomenon can be observed at the center of the nanosecond laser action zone<sup>[17]</sup> and molten splatters can be observed around the action area<sup>[18]</sup>. Fig. 3(a) is a laser damage diagram of an energy flux of 1.34 J/cm<sup>2</sup>. As can be seen from the

figure, the damaged area is elliptical due to the slight tilt of the focused beam relative to the target's plane. The laser damage points show annular regions of different colors, indicating that as the Gaussian laser energy flux distribution changes from the center to the edge, different physical processes occur on the Si surface. Possible damage mechanisms include ablation, sintering and oxidation/amorphization, etc.<sup>[5]</sup>. Fig. 3(b) is a laser damage diagram of an energy flux of 11.6 J/cm<sup>2</sup>. The laser-affected zone is essentially circular. The ablation zone and the sintering zone can still be observed and the ablation zone is obviously enlarged and sintered. The width of the area remains essentially the same. When the laser energy flux was greater than or equal to 10.3 J/cm<sup>2</sup>, the oxidized/amorphous region could not be observed, indicating that under this condition, the laser energy flux at the edge of the spot had exceeded the threshold of the oxidation/amorphization process.

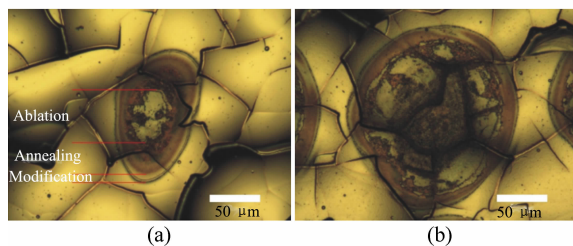


Fig. 3 Micrograph of Si-base multi-layer film irradiated by femtosecond single-pulse laser with energy densities of (a) 1.34 J/cm<sup>2</sup> and (b) 11.6 J/cm<sup>2</sup>

图 3 能量密度为(a) 1.34 J/cm<sup>2</sup>和(b) 11.6 J/cm<sup>2</sup>的单脉冲激光辐照硅基多层膜显微图

##### 3.1.2 Comparison of different laser energy flux irradiation morphology

In order to further study the evolution of the femtosecond laser ablation effect from laser energy fluxes, the long and short axis lengths of different laser energy flux irradiation damage areas were measured and plotted as curves, as shown in Fig. 4. The ablation zone size basically increased linearly with

the laser energy flux, a trend similar to that of the 532 nm nanosecond laser ablation polysilicon<sup>[19]</sup>. During the experiment, the minimum irradiation energy flux was  $0.076 \text{ J/cm}^2$  and no irradiation trace was observed corresponding to the irradiated surface, so the irradiation area was set to  $0 \text{ }\mu\text{m}$ . It can be seen from Fig. 4 that the changes in the long and short axes of the ablated region are basically the same and that there are two distinct growth trends of grown in the size of the ablated region as energy flux increases. For example: (1) In the range of  $0.076 - 1.01 \text{ J/cm}^2$ , the long axis of the ablation region increases rapidly from  $0 \text{ }\mu\text{m}$  to  $128 \text{ }\mu\text{m}$  (slope is 137); (2) in the range of  $1.01 - 24.7 \text{ J/cm}^2$ , the long axis of the ablated region increases from  $128 \text{ }\mu\text{m}$  to  $377 \text{ }\mu\text{m}$  (slope is 9.48). The difference in slope is a result of the spatial distribution of the pulse energy. The output waveform of the Ti:Sapphire femtosecond laser is generally quasi-Gaussian and the spatial distribution of the energy will dictate the morphology of the ablation in the film (including the ablation depth) or the damage effect. Ultra-laser energy flux irradiation experiments on the polished single crystal silicon surface (experimental results not shown) show that in the range of  $0.022 - 1.24 \text{ J/cm}^2$ , single pulse irradiation can only form a small diameter of  $7 - 100 \text{ }\mu\text{m}$  in the center of the spot. At a laser energy flux greater than  $1.24 \text{ J/cm}^2$ , the ablation effect can be observed gradually increasing on the irradiated surface (slope of 17.4). Comparing the results of single crystal silicon irradiation experiments, it can be inferred that in the range of  $0.076 - 1.01 \text{ J/cm}^2$ , oxidation and/or amorphization play a dominant role in the damage effect of Si-based multi-layer film materials; while within the  $1.01 - 24.7 \text{ J/cm}^2$  range, laser ablation plays a dominant role in material damage effects. According to the damage threshold definition<sup>[20-21]</sup>, the maximum laser energy flux at which no damage is observed and the average of the minimum laser

energy flux at which damage is observed can be taken as the damage threshold. The surface damage threshold under the current conditions of this experiment can be calculated to be  $0.543 \text{ J/cm}^2$ , which is equivalent to the damage threshold of the femtosecond laser for single crystal silicon reported in other literature<sup>[11,13]</sup>.

In addition, as the laser energy increases, the ablated region gradually become more circular and the laser damage and ablated regions gradually grow, even exceeding the size of the spot. During the laser irradiation experiment, it was found that when the single pulse energy exceeds  $6.24 \text{ J/cm}^2$ , plasma flash can be detected, which then becomes stronger as the energy is increased. This phenomenon is basically synchronous with the gradual rounding and enlargement of the damaged area observed by the microscope. Therefore, by comparing the effects of different laser energy flux damage, it is deduced that in the range of  $1.01 - 6.24 \text{ J/cm}^2$ , the main portion of Si-based multi-layer film damage is due to the absorption of non-thermal laser energy; in the range of  $6.24 - 24.7 \text{ J/cm}^2$ , this is mainly caused by laser-induced plasma ablation damage.

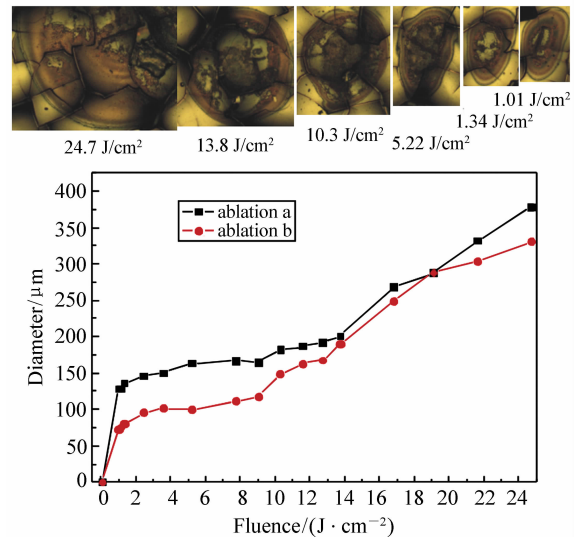


Fig. 4 Laser ablated zone sizes vary with pulse fluence

图4 烧蚀区域尺寸随脉冲能量的变化规律

### 3.2 Study on the Deep Damage Effect

#### 3.2.1 High Laser Energy Flux Single Pulse Stress Damage

When the single-pulse laser energy flux reaches  $2.42 \text{ J/cm}^2$  or more, the laser irradiation has some probability of causing deep damage to the Si-based multi-layer film. This damage effect is shown in Fig. 5. The main aspect of this damage is the sheet-like peeling of the film. The underlying single crystal silicon substrate and the green polycrystalline silicon film under visible light irradiation can be observed on the surface of the sample after peeling off the film layer. At the same time, sheet-like peeling and cracking can be observed on the surface of the substrate and polysilicon due to stress but no common thermal damage is observed from the continuous laser or the long pulse laser. Therefore, the main mechanism that causes the femtosecond laser to damage the Si-based multi-layer film is the stress damage caused by laser-induced shock waves.

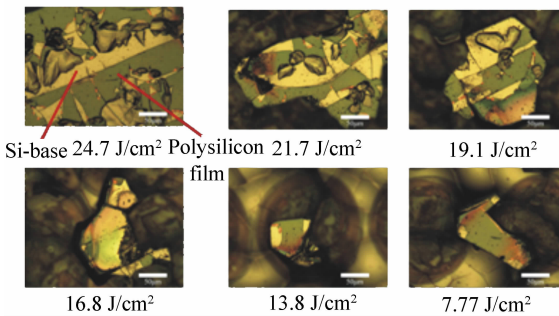


Fig. 5 Stress-induced damage at different pulse fluences

图 5 不同激光能量通量下应力损伤效果图

As the energy flux of the irradiated laser decreases, the area and probability of exfoliation decrease. By recording the number of times the sheet peels in 100 irradiation points, the variation of the damage with respect to the laser energy flux was calculated, as shown in Fig. 6. It can be seen from Fig. 6 that the laser energy flux is in the range of  $2.42 - 24.7 \text{ J/cm}^2$ , the stress damage probability increases linearly with the laser energy flux and the damage probability increases from 1% to 51%. Re-

ferring to the Optical Surface Laser Damage Threshold Test Method (GB/T 16601-1996), the threshold for stress damage in the Si-based multi-layer film using a femtosecond laser single pulse under pre-existing conditions can be calculated to be  $2.16 \text{ J/cm}^2$ . Previous studies have shown that there is a probable relationship between the destruction of the film and the size of the laser beam spot. The larger the spot, the greater the probability of destruction, and vice versa<sup>[20]</sup>. The effect of the spot on film destruction is related to the impurities and defects of the film. A defect is more likely to absorb laser energy, resulting in an uneven distribution of temperature or stress in the spot, which is ideal for ablation damage. For identical films, the larger the spot size, the higher the number of defects contained in the spot, and the more likely there is to be damaged. In this experiment, the relationship between the size of the ablated area and the stress damage probability with respect to laser energy flux can be found in Fig. 4 and Fig. 6, wherein the rate of change and threshold range of the two are essentially identical, further confirming the relationship between the probability of stress failure and the size of the ablated region.

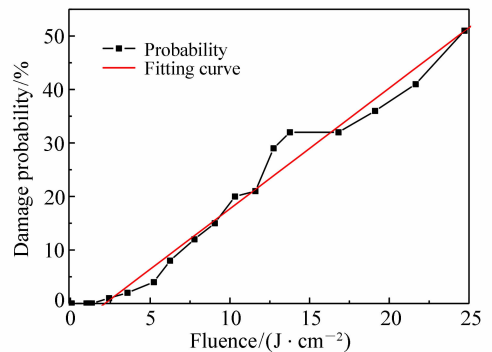


Fig. 6 Stress-induced damage probability varies with pulse fluence

图 6 应力损伤概率随激光能量通量的变化规律

#### 3.2.2 Low laser energy flux ablation cumulative damage

In order to study the failure mechanism of fem-

tosecond pulsed lasers on Si-based multi-layer film, the lowest laser energy flux that produces observable ablation ( $1.01 \text{ J/cm}^2$ ) was used to irradiate the same location multiple times to investigate the destructive effect of multiple pulse accumulation. The experimental results are shown in Fig. 7. The number of irradiation pulses were 1, 2, 4, 8, 16, 32, 64, 128, 256, and 512. As the number of pulses increased, the center of the ablated region became darker, indicating that the ablation depth was gradually increasing. By comparison, it was found that under continuous laser energy flux irradiation, the size of the ablated region of each sample remained essentially the same. When the number of pulses reached 512, the single crystal silicon substrate

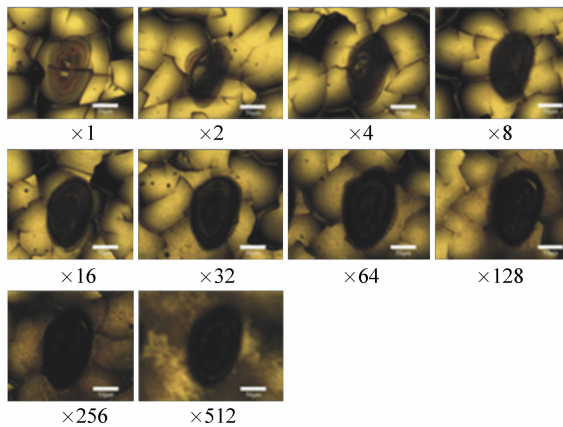


Fig. 7 Images of damage from continuous pulse ablation with fluence of  $1.01 \text{ J/cm}^2$

图7 低激光能量通量( $1.01 \text{ J/cm}^2$ )连续烧蚀效果图像

could be observed in the ablation center and a large amount of ablated particles were deposited around the ablation region. This result indicates that the main mechanism of Si-based multi-layer film damage under continuous irradiation at lower laser energy flux is the cumulative effect of surface ablation, and no obvious stress damage is observed.

## 4 Conclusion

In this paper, the damage characteristics of femtosecond pulsed lasers on Si-based multi-layer film was studied. The damage effect and mechanism of Si-based multi-layer film under different laser energy fluxes and different pulse accumulations were discussed. The experimental results showed that when the incident laser's single-pulse energy flux was in the range of  $1.01 \text{ J/cm}^2$  to  $24.7 \text{ J/cm}^2$ , obvious surface damage could be observed on the surface of Si-based multi-layer film depending on whether the laser energy flux distribution was low or high. The observed damage mechanisms were oxidation/amorphization, energy deposition and laser-induced plasma ablation. When the single-pulse laser energy flux reached  $2.16 \text{ J/cm}^2$  or more, laser irradiation had a probability causing deep damage or the Si-based multi-layer film where the damage was the overall peeling of the surface sheet layer caused by laser-induced stress. Continuous irradiation with low laser energy flux ( $\leq 1.01 \text{ J/cm}^2$ ) pulses could increase the ablation depth but avoid stress damage.

——中文对照版——

## 1 引言

硅基材料在可见和近红外波段光电成像等领域具有广泛的应用。研究不同参数激光对硅基材料的损伤破坏效应与机理具有十分重要的应用价值。激光造成硅基材料的损伤,可以表现为热效

应、力学效应以及电场效应等<sup>[1-4]</sup>。在超短脉冲激光与硅基材料的相互作用研究领域,国内外已经开展了不少辐照损伤效应的理论和实验研究。2002年, Bonse 等人研究了飞秒激光烧蚀的硅修饰阈值和形貌变化,发现随着激光能量通量的增加,材料表面将发生无定形化、熔化、重结晶、有核蒸发和烧蚀等一系列现象<sup>[5]</sup>。2004年, Jia 等人

研究了飞秒激光对单晶硅薄膜的作用,结果表明当激光作用强度低于烧蚀阈值时,足够的热量仍可导致硅材料无定形化<sup>[6]</sup>。2005年,Amer等人对比了飞秒和纳秒激光加工硅晶片诱导的应力和结构变化<sup>[7]</sup>。2008年,郭春风等人研究了超短脉冲激光辐照硅膜的热弹性<sup>[8]</sup>。2008年,Crawford等人研究了激光照射金属、氧化层和硅组成的多层膜的损伤过程,通过横截面检测发现处于内部的硅已经损伤而表面的保护层金属完好无损<sup>[9]</sup>。2011年,杨宏道等人研究了不同气体环境下纳秒脉冲激光诱导的硅表面特性变化规律,讨论了激光脉冲累积对硅材料形貌的影响机制<sup>[10]</sup>。2012年,Rublack等人采用 20 fs 至 2 000 fs 之间的脉冲激光照射表面镀有不同透明材料的硅片,利用光谱分析、原子力显微镜、扫描电镜、透射电镜等研究其损伤机制。结果表明损伤机制源于超短脉冲激光在硅层表面区域产生的电子空穴等离子体<sup>[3]</sup>。2013年,马鹏飞等人研究了不同激光能量通量的飞秒激光辐照对单晶硅的影响<sup>[11]</sup>。2014年,齐立涛测量了真空条件下不同波长纳秒激光对单晶硅的损伤能量阈值<sup>[12]</sup>。同年,邵俊峰等人理论研究了飞秒激光对硅热损伤和非热损伤机理,并分析了飞秒激光积累损伤效应<sup>[13]</sup>。

然而,使用的激光参数和硅基材料的制备方法不同,得到的损伤阈值与机理也不尽相同,特别是针对典型探测器膜层结构激光辐照特性和损伤机理的报道仍相对较少<sup>[14]</sup>。在前期工作中,本实验室已详细研究了电荷耦合器件(CCD)在超快激光辐照下的损伤和失效机理<sup>[15-16]</sup>,但是 CCD 膜层结构与超快激光相互作用物理机制尚未完全明确。

基于以上考虑,本文开展了硅基多层膜在飞秒脉冲激光辐照下的损伤效应试验研究,重点分析了飞秒脉冲激光辐照硅基多层膜的损伤机理,以及各种损伤效应对应的激光能量通量范围和阈值条件。

## 2 实验

实验采用电子束沉积方法制备的硅基多层膜作为研究对象。硅基多层膜各个膜层的厚度和成

份参照典型背照式 CCD 感光区参数进行简化设计,如图 1 所示。选取厚度为 2 mm 的(100)晶面单晶硅为基底,高纯硅(纯度 99.999% ~ 99.999 9%)为膜料,在镀膜真空度为  $3 \times 10^{-3}$  Pa 的条件下,依次沉积 300 nm 多晶硅、200 nm 二氧化硅和 15  $\mu\text{m}$  单晶硅。

图 2 显示了飞秒激光诱导损伤的实验装置示意图。本实验所使用的激光系统为超快 Ti:sapphire 放大器(Coherent Libra),输出激光的脉冲半高全宽为 50 fs,波长为 800 nm,重复频率为 1 kHz 或单触发,最大单脉冲能量约为 4 mJ,光束能量分布接近高斯分布。使用一对格兰棱镜和半波片将激光能量衰减到需要的量级,并用能量计进行监视。最后,利用一个离轴抛面反射镜将激光束聚焦到样品表面,光斑直径约为 100  $\mu\text{m}$ 。样品固定在可电脑编程控制的三维平移台上,保证每个激光脉冲作用在全新面上。实验过程中,每调整一次激光能量,作用 100 个烧蚀点,用以计算损伤概率。

实验采用金相显微镜对膜层表面损伤进行观察,所用检测设备为台湾奕叶国际有限公司 EB-4 金相显微镜,系统总放大倍率为 400 倍。

## 3 实验结果及分析

### 3.1 面烧蚀损伤效应研究

#### 3.1.1 典型辐照损伤形貌对比

图 3 显示了单脉冲激光辐照硅基多层膜表面的损伤效果显微图,在整个可调谐的能量范围内,未观察到明显的热熔损伤现象,证实飞秒激光具有非热烧蚀特性,这与纳秒等长脉冲激光作用效果明显不同,通常纳秒激光作用区中心可观察到熔融现象<sup>[17]</sup>,作用区域周围可观察到熔融喷溅物<sup>[18]</sup>。图 3(a)为能量通量 1.34 J/cm<sup>2</sup> 的激光损伤效果图。从图中可以看到,损伤区域为椭圆形,这是由于聚焦光束相对靶平面略微倾斜导致的。激光损伤点显示出不同颜色的环形区域,表明随着高斯激光能量通量从中心到边缘由高到低分布,在 Si 表面发生了不同的物理过程,可能的损伤机制包括烧蚀、烧结和氧化/无定形化等<sup>[5]</sup>。图 3(b)为能量通量 11.6 J/cm<sup>2</sup> 的激光损伤效果



图,激光影响区域基本呈圆形,仍可在图中观察到烧蚀区、烧结区,并且烧蚀区域明显扩大,但烧结区域宽度基本保持不变。当激光能量通量大于等于  $10.3 \text{ J/cm}^2$ ,已经无法观察到氧化/无定形区。说明在该条件下,光斑边缘的激光能量通量已经超过氧化/无定形化过程的阈值。

### 3.1.2 不同激光能量通量辐照形貌对比

为进一步研究飞秒激光烧蚀效应随激光能量通量的演化规律,测量了不同激光能量通量辐照损伤区域的长轴和短轴长度,并绘制成曲线,如图4所示。烧蚀区域尺寸基本随激光能量通量线性增长,这一趋势与  $532 \text{ nm}$  纳秒激光烧蚀多晶硅的实验结果相似<sup>[19]</sup>。实验过程中,最小辐照激光能量通量为  $0.076 \text{ J/cm}^2$ ,对应辐照表面观察不到任何辐照痕迹,因此设其辐照区域尺寸为  $0 \text{ }\mu\text{m}$ 。从图4中可以看出,烧蚀区域长短轴尺寸变化基本一致,烧蚀区域尺寸随着能量通量增加存在两个明显不同的增长趋势,即,(1)在  $0.076 \sim 1.01 \text{ J/cm}^2$  范围内,烧蚀区域长轴从  $0 \text{ }\mu\text{m}$  快速增大到  $128 \text{ }\mu\text{m}$  (斜率为 137);(2)在  $1.01 \sim 24.7 \text{ J/cm}^2$  范围内,烧蚀区域长轴从  $128 \text{ }\mu\text{m}$  增大到  $377 \text{ }\mu\text{m}$  (斜率为 9.48)。烧蚀区域尺寸增长的斜率不同是由脉冲能量的空间分布所致,钛宝石飞秒激光的输出波形一般为准高斯型,其能量的空间分布将主导薄膜烧蚀的形貌(包括烧蚀深度)或损伤效应。对抛光单晶硅表面更加细致的低激光能量通量辐照实验表明(结果未显示在文中),在  $0.022 \sim 1.24 \text{ J/cm}^2$  范围内,单脉冲辐照仅能在光斑中心位置形成轻微的直径  $7 \sim 100 \text{ }\mu\text{m}$  的氧化/无定形化(斜率为 329)区域;激光能量通量大于  $1.24 \text{ J/cm}^2$ ,才能在辐照表面观察到随辐照激光能量通量增强而逐渐明显的烧蚀效应(斜率为 17.4)。对比单晶硅辐照实验结果可推测,在  $0.076 \sim 1.01 \text{ J/cm}^2$  范围内,氧化和/无定形化在硅基多层膜材料损伤效应中占主导作用;而在  $1.01 \sim 24.7 \text{ J/cm}^2$  范围内,激光烧蚀在材料损伤效应中占主导作用。根据损伤阈值定义<sup>[20-21]</sup>,可取未观察到损伤的最大激光能量通量和观察到损伤的最小激光能量通量的平均值作为损伤阈值,则可计算出本次实验在现有条件下的表面损伤阈值  $0.543 \text{ J/cm}^2$ ,这一数值与其他文献报道的飞秒

激光对单晶硅的损伤阈值基本相当<sup>[11,13]</sup>。

另外,随着激光能量增加,烧蚀区域长轴和短轴尺寸逐渐接近,烧蚀区域形状更接近圆形,激光损伤和烧蚀区域逐渐增大,甚至超过光斑尺寸。在激光辐照实验过程中发现,当单脉冲能量超过  $6.24 \text{ J/cm}^2$  时,可探测到等离子体闪光,并随着能量增强而变强,这一现象与显微镜观察到的损伤区域逐渐变圆和变大基本是同步的。因此,通过对比不同激光能量通量损伤效果可初步判定,在  $1.01 \sim 6.24 \text{ J/cm}^2$  范围内,硅基多层膜主要损伤机制为膜层吸收激光能量诱导的非热烧蚀损伤;而在  $6.24 \sim 24.7 \text{ J/cm}^2$  范围内,主要是由激光诱导等离子体引起的表面烧蚀损伤。

## 3.2 深层损伤效应研究

### 3.2.1 高激光能量通量单脉冲应力损伤

当单脉冲激光能量通量达到  $2.42 \text{ J/cm}^2$  以上,激光辐照有一定几率造成硅基多层膜的深层损伤,损伤效果如图5所示。损伤的主要现象是膜层的片状剥离,膜层剥离后的样品表面可观察到底层单晶硅衬底和在可见光照射下显绿色的多晶硅膜。同时,在衬底和多晶硅表面可观察到由于应力作用引起的片状剥离和裂纹,而未观察到类似连续激光或长脉冲激光辐照条件下常见的热损伤。因此可判断导致飞秒激光单脉冲损伤硅基多层膜的主要损伤机制为激光诱导冲击波导致的应力损伤。

随辐照激光能量通量降低,片状剥离的面积和几率都相应降低。通过记录 100 个辐照点发生片状剥离的次数,计算出了损伤概率随激光能量通量的变化规律,如图6所示。从图6中可以看出,激光能量通量在  $2.42 \sim 24.7 \text{ J/cm}^2$  范围内,应力损伤概率基本上随激光能量通量线性增长,损伤概率由 1% 增长到 51%。参照《光学表面激光损伤阈值测试方法 GB/T 16601-1996》,可计算在现有条件下飞秒激光单脉冲造成硅基多层膜应力损伤的阈值条件为  $2.16 \text{ J/cm}^2$ 。之前的研究结果已经表明,薄膜的破坏与激光束光斑大小的关系带有明显的几率性,光斑越大则破坏的几率越大,反之,破坏几率越小<sup>[20]</sup>。薄膜破坏的光斑效应与薄膜的杂质缺陷有关,缺陷更容易吸收激光能量导致光斑内温度场或应力场分布不均并发生优先

烧蚀破坏。同一块薄膜,光斑越大,光斑内包含的缺陷数越高,越容易引起破坏。在本实验中,综合图 4 和图 6 中烧蚀区域尺寸和应力损伤概率随激光能量通量的变化规律可以发现,两者的变化趋势和阈值范围基本相同,进一步证实应力破坏概率与烧蚀区域尺寸存在明显的对应关系。

### 3.2.2 低激光能量通量烧蚀累积损伤

为研究飞秒脉冲激光对硅基多层膜的破坏机理,采用可观察到烧蚀效应的最低激光能量通量 ( $1.01 \text{ J/cm}^2$ ) 连续多次辐照同一位置,考察多次脉冲累积的破坏效应。实验效果如图 7 所示,辐照脉冲数分别为 1、2、4、8、16、32、64、128、256 和 512。通过对比发现,在该激光能量通量连续辐照下,各样品烧蚀区域尺寸基本保持不变,随着脉冲数增加,烧蚀区域中心颜色明显变深。这说明随着烧蚀深度的逐渐增加,当脉冲数达到 512 时,烧蚀中心可观察到单晶硅衬底,并且烧蚀区周围沉积了大量回落的烧蚀产物颗粒。这一结果表明,在较低激光能量通量连续辐照下的硅基多层膜损

伤的主要机制为表面烧蚀的累积效应,未观察到明显的应力破坏。

## 4 结 论

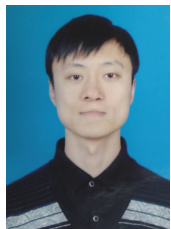
本文研究了飞秒脉冲激光对硅基多层膜的损伤特性,重点讨论了硅基多层膜在不同激光能量通量和不同脉冲累积下的损伤效应与机理。实验结果分析表明,当入射激光单脉冲能量通量在  $1.01 \text{ J/cm}^2$  到  $24.7 \text{ J/cm}^2$  范围内,可在硅基多层膜表面观察到明显的表面损伤,根据激光能量通量分布由低到高,其损伤机制依次为氧化/无定形化、能量沉积和激光诱导等离子体烧蚀等。当单脉冲激光能量通量达到  $2.16 \text{ J/cm}^2$  以上,激光辐照有一定几率造成硅基多层膜的深层损伤,损伤机制为激光诱导应力导致的表面片状膜层的整体剥离。采用低激光能量通量 ( $\leq 1.01 \text{ J/cm}^2$ ) 脉冲进行连续辐照,可增加烧蚀深度,但未能造成应力损伤。

## References:

- [1] FEDOSEJEVS R, KIRKWOOD S E, HOLENSTEIN R. Femtosecond interaction processes near threshold: damage and ablation[J]. *Proceedings of SPIE*, 2007, 6403: 640302.
- [2] CRAWFORD T H R, YAMANAKA J, BOTTON C A. High-resolution observations of an amorphous layer and subsurface damage formed by femtosecond laser irradiation of silicon[J]. *Journal of Applied Physics*, 2008, 103(5): 053104.
- [3] RUBLACK T, HARTNAUER S, MERGNER M. Mechanism of selective removal of transparent layers on semiconductors using ultrashort laser pulses[J]. *Proceedings of SPIE*, 2012, 8247: 82470Z.
- [4] 王涛涛, 付跃刚, 汤伟, 等. 单 CCD 彩色相机激光干扰模型及外场干扰实验[J]. *发光学报*, 2015, 36(5): 588-594. WANG T T, FU Y G, TANG W, *et al.*. Laser jamming model and out-field laser jamming experiment of single CCD colour imaging system[J]. *Chinese Journal of Luminescence*, 2015, 36(5): 588-594. (in Chinese)
- [5] BONSE J, BAUDACH S, KRÜGER J, *et al.*. Femtosecond laser ablation of silicon modification thresholds and morphology[J]. *Applied Physics A*, 2002, 74(1): 19-25.
- [6] JIA J, LI M, THOMPSON C V. Amorphization of silicon by femtosecond laser pulses[J]. *Applied Physics Letters*, 2004, 84(16): 3025.
- [7] AMER M S, EL-ASHRY M A, DOSSER L R, *et al.*. Femtosecond versus nanosecond laser machining: comparison of induced stresses and structural changes in silicon wafers[J]. *Applied Surface Science*, 2005, 242(1-2): 162-167.
- [8] 郭春风, 于继平, 王德飞, 等. 超短脉冲激光辐照硅膜的热弹性[J]. *强激光与粒子束*, 2008, 20(6): 907-911. GUO CH F, YU J P, WANG D F, *et al.*. Thermoelasticity effect on Si film irradiated by ultra-short pulse laser[J]. *High Power Laser and Particle Beams*, 2008, 20(6): 907-911. (in Chinese)
- [9] CRAWFORD T H R, YAMANAKA J, HSU E M. Femtosecond laser irradiation of metal and thermal oxide layers on silicon: studies utilising cross-sectional transmission electron microscopy[J]. *Applied Physics A*, 2008, 91(3): 473-478.
- [10] 杨宏道, 李晓红, 李国强, 等. 不同气体环境下 532 nm 激光诱导硅表面形貌的研究[J]. *中国光学*, 2011, 4(1): 86-92. YANG H D, LI X H, LI G Q, *et al.*. Surface morphology of silicon induced by 532 nm nanosecond laser under different

- ambient atmospheres[J]. *Chinese Optics*,2011,4(1):86-92. (in Chinese)
- [11] 马鹏飞,王克栋,常方高,等.不同能量密度的飞秒激光辐照对单晶硅的影响研究[J].*人工晶体学报*,2013,42(2):273-277.  
MA P F,WANG K D,CHANG F G,*et al.*. Effects of the irradiation on silicon by femtosecond laser of various energy densities[J]. *Journal of Synthetic Crystals*,2013,42(2):273-277. (in Chinese)
- [12] 齐立涛.真空条件下不同波长固体激光烧蚀单晶硅的实验研究[J].*中国光学*,2014,7(3):442-448.  
QI L T. Different wavelength solid-state laser ablation of silicon wafer in vacuum[J]. *Chinese Optics*,2014,7(3):442-448. (in Chinese)
- [13] 邵俊峰,郭劲,王挺峰.飞秒激光与硅的相互作用过程理论研究[J].*红外与激光工程*,2014,43(8):2419-2424.  
SHAO J F,GUO J,WANG T F. Theoretical research on dynamics of femto-second laser ablation crystal silicon[J]. *Infrared and Laser Engineering*,2014,43(8):2419-2424. (in Chinese)
- [14] 张震,周孟莲,张检民,等.CCD中的激光光斑阴影现象及机理[J].*光学精密工程*,2013,21(5):1365-1371.  
ZHANG ZH,ZHOU M L,ZHANG J M,*et al.*. Shadows of laser spots in CCD and their mechanism[J]. *Opt. Precision Eng.*,2013,21(5):1365-1371. (in Chinese)
- [15] 邵俊峰,刘阳,王挺峰,等.皮秒激光对电荷耦合器件多脉冲损伤效应研究[J].*兵工学报*,2014,35(9):1408-1413.  
SHAO J F,LIU Y,WANG T F,*et al.*. Damage effect of charged coupled device with multiple-pulse picosecond laser[J]. *Acta Armamentarii*,2014,35(9):1408-1413. (in Chinese)
- [16] 王明,王挺峰,邵俊峰.面阵CCD相机的飞秒激光损伤分析[J].*中国光学*,2013,6(1):96-102.  
WANG M,WANG T F,SHAO J F. Analysis of femtosecond laser induced damage to array CCD camera[J]. *Chinese Optics*,2013,6(1):96-102. (in Chinese)
- [17] 张健,林广平,张睿,等.准分子激光相位掩模法制备大晶粒尺寸多晶硅薄膜[J].*光学精密工程*,2012,20(1):58-63.  
ZHANG J,LIN G P,ZHANG R,*et al.*. Fabrication of large grain size p-Si film by phase modulated excimer laser crystallization[J]. *Opt. Precision Eng.*,2012,20(1):58-63. (in Chinese)
- [18] 冯爱新,庄绪华,薛伟,等.1064 nm、532 nm、355 nm 波长脉冲激光辐照多晶硅损伤特性研究[J].*红外与激光工程*,2015,44(2):461-465.  
FENG A X,ZHUANG X H,XUE W,*et al.*. Damage characteristics of polysilicon under wavelengths of 1064 nm, 532 nm and 355 nm laser irradiation[J]. *Infrared and Laser Engineering*,2015,44(2):461-465. (in Chinese)
- [19] 韩振春,薛伟,冯爱新,等.不同波长的纳秒脉冲激光对多晶硅损伤特性研究[J].*应用激光*,2013,33(3):313-317.  
HAN ZH CH,XUE W,FENG A X,*et al.*. A Different wavelength of nanosecond pulse laser damage characteristics of polycrystalline silicon research[J]. *Applied Laser*,2013,33(3):13-317. (in Chinese)
- [20] 孙承伟,陆启生,范正修,等.激光辐照效应[M].北京:国防工业出版社,2002.  
SUN CH W,LU Q SH,FAN ZH X,*et al.*. *Laser Irradiation Effect*[M]. Beijing:National Defense Industry Press,2002. (in Chinese)
- [21] 徐斌,伍晓宇,罗烽,等.0Cr18Ni9 不锈钢箔的飞秒激光烧蚀[J].*光学精密工程*,2012,20(1):45-51.  
XU B,WU X Y,LUO F,*et al.*. Ablation of 0Cr18Ni9 stainless steel films by femtosecond laser[J]. *Opt. Precision Eng.*,2012,20(1):45-51. (in Chinese)

#### 作者简介:



ZHENG Changbin(1981—), male, Fujin, Heilongjiang, Ph. D., Associate Researcher, B. S. in physics, college of physics, Jilin Univeristy, 2001 – 2005; Ph. D in optics, department of physics, Harbin Institute of Technology, 2005 – 2011 is mainly engaged in research on the effects of laser irradiation. E-mail:zhengchangbin@ciomp. ac. cn

郑长彬(1981—),男,黑龙江富锦人,博士,副研究员,2005年于吉林大学获得硕士学位,2011年于哈尔滨工业大学获得博士学位,主要从事激光辐照效应方面的研究。E-mail:zhengchangbin@ciomp. ac. cn